ACS OMEGA

http://pubs.acs.org/journal/acsodf

Article

Schiff-Based Metal Complexes of Lamotrigine: Design, Synthesis, Characterization, and Biological Evaluation

Saima Najm,* Humaira Naureen, Kishwar Sultana, Fareeha Anwar, Muhammad Mubbashir Khan, Humaira Nadeem, and Muhammad Saeed*

Cite This: *ACS Omega* 2021, 6, 7719−7730

Read Online

ACCESS | Metrics & More | Article Recommendations | Supporting Information

ABSTRACT: In the current study, a series of Schiff base derivatives of lamotrigine are complexed with zinc, copper, silver, and tin and characterized by spectroscopic techniques and biological assays. Docking analyses revealed six complexes with favorable binding interactions, which were further subjected to *in vitro* anticancer activity. The complexes **6b** and **6c** displayed the most potent antiproliferative activity against MCF-7 cell lines with an IC_{50} value of 11.9 ± 0.27 and 12.0 ± 0.14 μM, respectively, as compared with the standard doxorubicin with an IC_{50} value of 0.90 ± 0.14 μM. *In vivo* anticonvulsant activities of the compounds were evaluated by the subcutaneous pentylenetetrazole model and neurotoxic activities by the minimal motor impairment model. The neurotoxicity of targeted compounds was measured using the rotating rod (ROT) method. Computational studies were carried out using the reported crystal structures of multidrug-resistant protein (PDB-ID: 2KAV) and dihydrofolate reductase (PDB-ID: 3GHW), indicating that the compound **6c** showed significant interactions at the voltage-gated sodium ion channel in the brain and at dihydrofolate reductase enzyme in the breast. Certain metal complexes of Schiff base ligands (e.g., **6c**) were found to possess the most potent anticancer, anticonvulsant, and neurotoxic potential than lamotrigine alone.

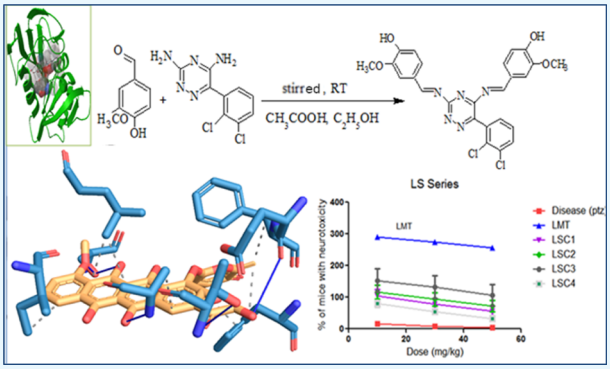

1. INTRODUCTION

Lamotrigine [3,5-diamino-6-(2, 3-dichlorophenyl)-1,2,4-triazine] (LTG) is a novel antiepileptic drug, which is chemically unique when compared with other anticonvulsants.[1] It is used to control seizures, convulsions of various grades, and bipolar disorders.[2] The antiepileptic effect of LTG entails its binding with the voltage-gated sodium channels (VNaC)[3,4] and thus inhibiting the release of endogenous amino acids and acetylcholine. LTG can also be used as an anticancer drug against colon cancer (COLO 320 HSR) and chronic myelogenous leukemia (K562).[5] Furthermore, LTG shows strong antiproliferative activity in breast cancer cells, as demonstrated in both *in vitro* and *in vivo* studies.[6] LTG in low doses can increase the protective index of felbamate against seizures by enhancing the anticonvulsant effect without a significant increase in neurotoxicity.[7]

Data from various studies have demonstrated that LTG is medicinally less potent than other anticonvulsants and exhibits greater side effects. The frequent common side effect of LTG, as experienced by various patients, is hepatoxicity.[8] To increase potency and/or to minimize side effects, LTG has been extensively derivatized to other analogues.[2] For instance, oxo-analogues of LTG have been synthesized to enhance anticoccidial and herbicidal activities.[9] Additionally several series of structurally diverse analogues of LTG were prepared and tested for their antibacterial activity against Gram-negative bacteria.[10]

Schiff bases (SB) are considered to be a versatile pharmacophore for drug design and development of many bioactive compounds. Especially when complexed with transition metals, they play important roles in industrial, herbicidal, anticancer, antifungal, and antibacterial applications.[11] After the discovery of the metal-based anticancer drug (cisplatin), the medicinal use of drugs with metal complex has gained impetus.[12]

Applications of SB−metal complexes as chemical nucleases are the focus of current research. Inspired by the interesting biological activities, SB derivatives of LTG were synthesized for this study and later on treated with Zn, Cu, Ag, and Sn to afford lamotrigine−SB−metal (LTG−SB−M) complexes. After characterization by various spectroscopic techniques,

Received: January 5, 2021
Accepted: March 2, 2021
Published: March 15, 2021

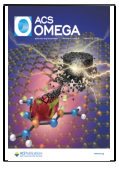

Scheme 1. General Scheme for the Synthesis of LTG−SB−M Complexes (4_{a-c}−7_{a-c})

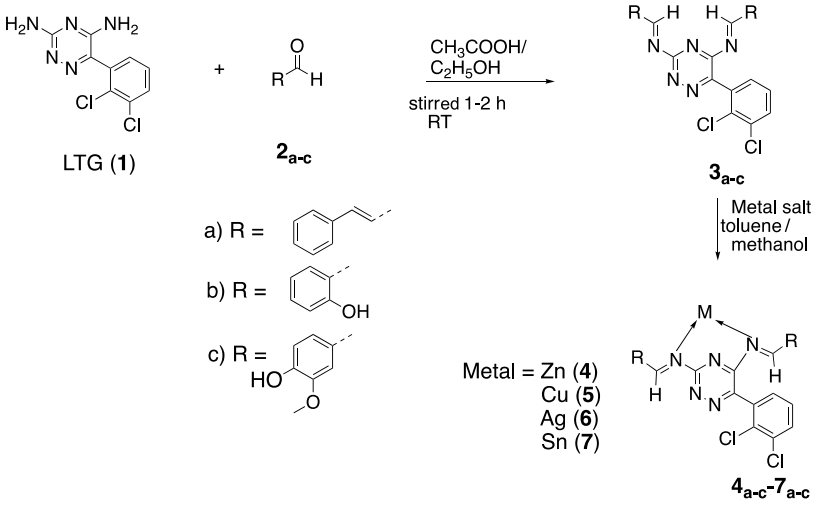

Table 1. Anticonvulsant Effects of LTG−SB−M Complexes in PTZ-Induced Convulsions in Mice[a]

compound	latency time (sec)	average duration of seizure (sec)	seizure score (counts)	mortality (counts)
4a	145.0 ± 23.4**	86.5 ± 5.0***	15.0 ± 4.9**	0.0
5a	170.0 ± 45.2**	81.5 ± 2.1***	11.0 ± 1.9**	0.0
6a	180.0 ± 75.9**	105 ± 7.1**	11.0 ± 2.3**	1
7a	220.0 ± 72.7***	110 ± 14.1**	12.0 ± 1.2**	0.0
4b	240.0 ± 10.3***	81.5 ± 2.1***	10.0 ± 6.5***	0.0
5b	250.0 ± 88.3***	97.5 ± 28.3***	11.0 ± 2.4**	1
6b	330.0 ± 67.8***	95 ± 10.5***	12.0 ± 1.8**	0.0
7b	190.0 ± 70.1**	99 ± 7.1***	12.0 ± 1.5**	0.0
4c	250.0 ± 10.3***	81.5 ± **1.5*****	14.0 ± 3.7**	0.0
5c	230.0 ± 70.1***	115 ± 10.0**	10.0 ± 2.6***	0.0
6c	376.7 ± **31.2*****	110 ± 11.6**	9.0 ± **0.8*****	**0.0**
7c	160.0 ± 49.0**	125 ± 15.3*	11.0 ± 1.6**	0.0
vehicle (V)	0.00	0.00	0.00	0.0
LTG control	211.7 ± 98.1***	90 ± 3.5***	11.0 ± 2.3***	0.0
PTZ control	98.0 ± 21.7	155 ± 1.4	21.0 ± 0.0	6

[a]Data are represented as mean ± SEM. n = 10. ***P < 0.001, **P < 0.01, and *P < 0.05 vs PTZ group as measure by One-Way Anova with Dunnett's post hoc test.

the complexes were computationally docked to various functional proteins to assess their potential to bind with the target enzyme/receptor. Concomitantly, *in vitro* (anticancer) and *in vivo* (anticonvulsant and neurotoxic) studies were conducted on the newly synthesized LTG−SB−M complexes considering the possibility of interactions with and attenuation of the VNaC in the brain.

2. RESULTS AND DISCUSSION

2.1. Chemistry. Synthesis of SB derivatives of LTG (**1**) was accomplished by reacting the amino group of **1** with cinnamaldehyde (**2a**), salicylaldehyde (**2b**), or vanillin (**2c**) in the presence of catalytic amounts of glacial acetic acid in ethanol. The reaction was stirred at room temperature for 1−2 h to afford SBs, 3_{a-c}, in excellent yields. The synthesis of metal coordinate complexes was achieved by reacting equimolar amounts of SB (3_{a-c}) and metal compound ($ZnCl_2$, $Cu(CH_3COO)_2{\cdot}H_2O$, $AgNO_3$, or $C_8H_{18}Cl_2Sn$) in the presence of toluene and triethylamine as catalysts as shown in Scheme 1. The reaction mixture was refluxed for several hrs to afford the synthesis of target LTG−SB−M complexes (4_{a-c}−7_{a-c}) in excellent yields. Structures of the LTG−SM−M complexes were elucidated using various spectroscopic techniques, such as FTIR, NMR, and mass spectrometry. The presence of metal in the complexes was ascertained by measuring atomic absorption spectra of the complexes.

The main absorption frequencies in FTIR showed strong symmetric and asymmetric bands due to −OH vibrations at 3500−3700 cm^{-1} and two bands assigned to −NH in the region of 3300−3500 cm^{-1} and 1600 cm^{-1}. For all compounds, the absorptions close to around 1080−1350 cm^{-1} were assigned to −C−N− (aromatic amine) stretching, and the absorptions around 1400−1600 corresponded to aromatic −C═C− stretching, whereas the absorption bands around 3000−3100 cm^{-1} direct the presence of aromatic −C−H stretching. These values for aromatic amine vibrational bands (−C−N) suggest that the imine acceptor electronic density shortens the −C−N− bond; the M−N bond appears in the range of 700−800 cm^{-1}, confirming the SB−M complex (Supporting Information, Figures S1−S15). Detailed IR data of the synthesized compounds are given in the Experimental Section. The structures of SBs (3_{a-c}) were confirmed by NMR and mass spectrometry; the ^{1}H NMR spectra of **3b** and **3c** exhibited a strong peak at approximately δ 9.5−10.6 ppm for

https://dx.doi.org/10.1021/acsomega.1c00027
ACS Omega 2021, 6, 7719−7730

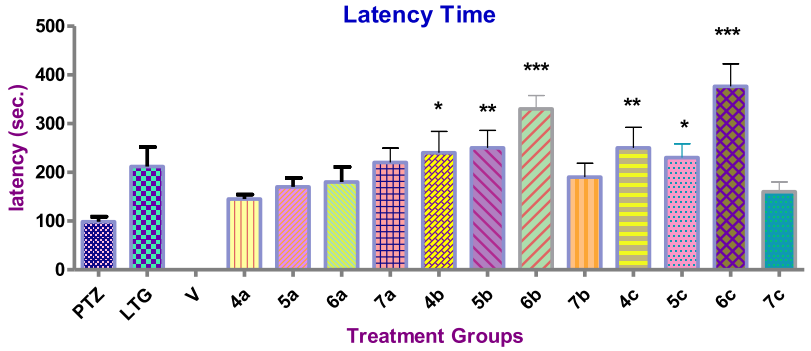

Figure 1. Attenuation of latency time of PTZ-induced seizures by different metal complexes of LTG. Data are represented as mean ± SEM; $n = 10$. ***$P < 0.001$, **$P < 0.01$, and *$P < 0.05$ vs PTZ group as measured by One-Way Anova with Dunnett's post hoc test.

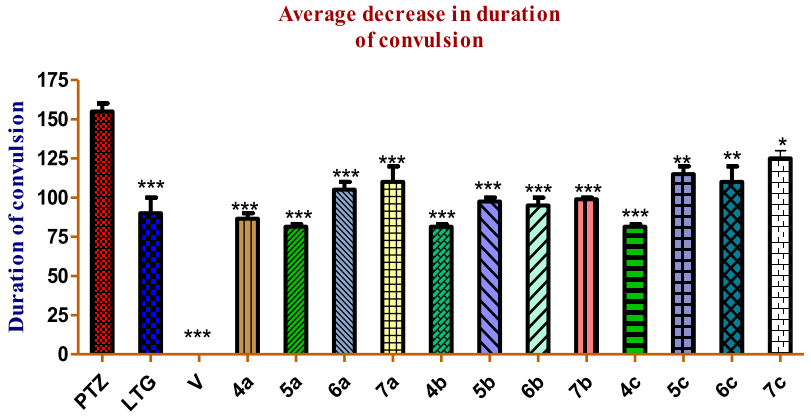

Figure 2. Decrease of duration of convulsions in PTZ-induced seizures by LTG−SB−M complexes. Data are represented as mean ± SEM, $n = 10$. ***$P < 0.001$, **$P < 0.01$, and *$P < 0.05$ vs PTZ group as measure by One-Way Anova with Dunnett's post hoc test.

−OH. The corresponding peak for **3a** was not observed due to the absence of −OH group (see the Supporting Information, Figures S16, S18, and S20 for ^{1}H NMR spectra). The amino proton (−NH) appeared at δ 7.36 and 7.70 ppm for **3a**, at δ 7.36 and 7.70 ppm for **3b**, and at δ 6.95 and 7.70 ppm for **3c**. The protons with respect to the triazine ring and nitrogen atom in **3a−c** exhibited no significant shifting in the ^{1}H NMR spectrum. ^{13}C NMR spectra of **3a−c** (see Supporting Information, Figures S17, S19, and S21) are in total agreement with the corresponding elucidated structures. A signal commonly assigned to the amide carbon atom was observed at about δ 131.10 ppm for **3a**, at δ 131.07 for **3b**, and at δ 131.08 ppm for **3c**, consistent with previous reports. The signal corresponding to the benzene ring appeared around δ 126, 128, and 129 ppm in **3a−c**, respectively. In the case of **3c**, the methyl group appears at δ 56 ppm. Mass spectra showed the correct molecular ions as suggested by their molecular formulae. Confirmation of the metal complexes of the SBs was ascertained by the atomic absorption spectroscopy as shown in the Supporting Information, Figures S22−S27.

2.2. Solubility Studies. After synthesis, the metal complexes were subjected to solubility studies showing that all compounds were highly soluble in DMSO, ethanol, and methanol at room temperature. The compounds showed poor solubility in chloroform, whereas they were sparingly soluble in water at room temperature. Molecular structures and their respective molecular data are presented in Table S1. The solubility values of various ligands and their metal complexes are given in Table S2.

2.3. Biological Activities of LTG−SB−M Complexes. *2.3.1. Anticonvulsant Activity.* Clonic convulsions were induced with an optimized intraperitoneal injection (70 mg/Kg) of pentylenetetrazole (PTZ) in mice, followed by the observation of latency time, seizure score, and reduction in the number of convulsions after the treatment with 5 mg/kg of the newly synthesized LTG−SB−M complexes. The results of the complexes were compared with the standard LTG drug and carrier (solvent) control. As shown in Table 1 and Figure 1, untreated mice showed seizures within 100 s, whereas LTG treatment prolonged the latency time of seizures up to ∼212 s after i.p. injection of PTZ.

All of the tested metal complexes of LTG SBs demonstrated significant enhancement of the latency time of PTZ-induced seizures in mice. When compared with the standard LTG drug, the latency time of PTZ-induced seizures were enhanced for **4b** (13%), **4c** (18%), **5b** (18%), **5c** (8%), **6b** (56%), **6c** (78%), and **7a** (4%); whereas for the remaining complexes, the latency times were not found to be better than that of LTG. The longest latency times of seizure initiation were observed for **6b** and **6c**, which prolonged the onset of seizures up to 330.0 ± 67.8 and 376.7 ± 31.2 s, respectively. Therefore, the silver complexes derived from the SBs of LTG and salicylaldehyde or vanillin yielded improved latency time in the PTZ-induced mouse epileptic model.

Duration of PTZ-induced convulsions was also found to be reduced significantly after the treatment with LTG−SB−M complexes. The positive control, LTG caused a significant decrease (42%) in the time duration of convulsions as compared to PTZ (negative control). Interestingly, all

https://dx.doi.org/10.1021/acsomega.1c00027
ACS Omega 2021, 6, 7719−7730

synthesized complexes also reduced the duration of convulsions from 19 to 47% when compared with the negative control, as shown in Table 1 and Figure 2. Three complexes, **4b**, **4c**, and **5a** showed significantly better anticonvulsant results, whereas the remaining complexes demonstrated comparatively inferior anticonvulsant activity than the positive control, LTG.

Another parameter that was interesting to observe was the attenuation of the convulsion score, which signifies the reduction in the number of PTZ-induced seizures in mice treated with LTG−SB−M complexes. The data in Table 1 and Figure 3 shows that LTG reduced the frequency of seizures up

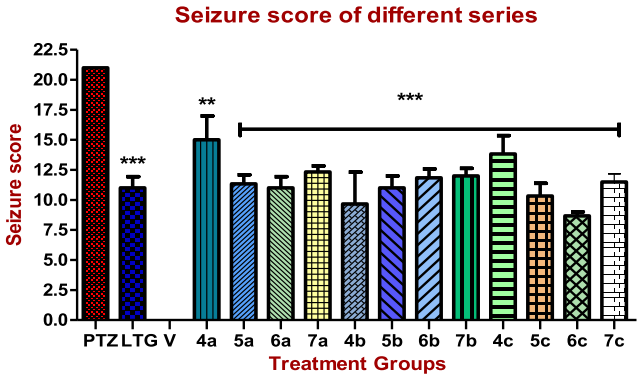

Figure 3. Determination of seizure score of PTZ-induced seizures by different metal complexes of LTG. Data are represented as mean ± SEM, $n = 10$. ***$P < 0.001$, **$P < 0.01$ vs PTZ group as measure by One-Way Anova with Dunnett's post hoc test.

to almost half. In the case of the synthesized LTG−SB−M complexes, similar reduction in the number of seizures was observed at a dose of 5 mg/kg. Among all tested compounds, the complex **6c** was observed to be the best complex by exhibiting ∼2.3 times less seizure score in the PTZ-induced mouse model as shown in Figure 3. The data mentioned in Table 1 represents 100% protection in all compounds (except **5b** and **6a**) at a dose of 5 mg/kg in the PTZ-induced mouse model. Compounds **5b** and **6a** show 90% protection against PTZ-induced convulsions.

2.3.2. Neurotoxicity Test (MMI). Neurotoxic effects of PTZ were measured by observing the motor coordination of the treated mice on a rotating rod for the duration of 5 min. Three different doses of PTZ were examined. With a PTZ dose of 10 mg/kg, the mice could stay on the rotating rod for an average duration of ∼17 s, which was decreased to ∼10 and ∼8 s with an increased PTZ dose of 30 and 50 mg/kg, respectively. When the mice were pretreated with 10, 30, and 50 mg/kg dose of the synthetic compounds, the neurotoxic effects of PTZ were significantly reduced and they demonstrated better motor coordinations. In the case of the LTG-treated positive control group, the residence time was enhanced up to 290.0 ± 16.7, 245.8 ± 15.4, and 200.7 ± 13.7 s, when treated with 10, 30, and 50 mg/kg dose of the drug, respectively. Among the synthetic compounds, the complex **7c** demonstrated the best neuroprotective effect, exhibiting a residence time enhancement up to 190.0 ± 74.6, 167.4 ± 89.8, and 140.5 ± 94.9 s, with a dose of 10, 30, and 50 mg/kg. Other synthetic compounds and complexes showed a similar trend as shown in Table 2.

2.3.3. Cytotoxicity Studies. The LTG−SB−M complexes were also tested for their anti-cancer potential. A fixed dose of

Table 2. Neurotoxicity of LTG−SB and LTG−SB−M Complexes in ROT Mice Model[a]

	time on Rod (sec)		
	dose (mg/kg)		
compound	10	30	50
3a	104.2 ± 76.4	80.9 ± 32.1	55.6 ± 12.3
4a	66.7 ± 15.1	45.4 ± 10.3	30.6 ± 4.2
5a	76.7 ± 19.7	55.9 ± 12.9	40.9 ± 10.7
6a	141.7 ± 102.5	120.0 ± 98.7	75.8 ± 20.3
7a	155.0 ± 97.5	130.6 ± 92.4	100.4 ± 87.7
3b	110.8 ± 98.6	90.5 ± 82.3	65.97 ± 54.9
4b	105.0 ± 98.5	80.6 ± 78.6	54.26 ± 42.3
5b	116.7 ± 94.3	100.0 ± 86.3	75.83 ± 54.3
6b	153.3 ± 92.7	146.3 ± 90.9	130.0 ± 91.7
7b	80.0 ± 27.6	68.9 ± 25.7	45.64 ± 19.3
3c	140.7 ± 92.4	126.4 ± 88.0	100.0 ± 82.3
4c	80.0 ± 75.3	50.6 ± 42.5	30.65 ± 25.7
5c	121.7 ± 98.3	90.0 ± 85.6	75.64 ± 52.7
6c	150.0 ± 97.0	135.7 ± 92.6	120.0 ± 90.5
7c	190.0 ± **74.6**	167.4 ± **89.8**	140.5 ± **94.0**
vehicle (cont)	300.0 ± 156.4	260.9 ± 124.3	240.6 ± 109.8
LTG	290.0 ± 16.7	245.8 ± 15.4	200.7 ± 13.7
PTZ	16.67 ± 8.165	10.46 ± 1.654	7.7 ± 2.4

[a]Data are represented as mean ± SEM. In each group, 10 mice were treated with the given dose of the tested compounds.

30 μM was used to test the growth inhibition effects in the cultured human mammary cancer MCF-7 cell line and compared with the standard doxorubicin as shown in Table 3. Apart from the compounds **6b** and **6c**, all tested complexes

Table 3. Cytotoxicity of LTG−SB−M Complexes in MCF-7 Cell Lines[a]

sample code	conc. (μM)	% inhibition/stimulation	IC50 ± SD
4a	30	0.00	inactive
5a	30	0.00	inactive
6a	30	0.00	inactive
7a	30	0.00	inactive
4b	30	0.00	inactive
5b	30	0.00	inactive
6b	**30**	**101.2**	11.9 ± 0.27
7b	30	0.00	inactive
4c	30	0.00	inactive
5c	30	0.00	inactive
6c	**30**	**99.9**	12.0 ± 0.36
7c	30	0.00	inactive
doxorubicin (DOX)	30	101.2	0.90 ± 0.14

[a]Data are presented as mean ± SEM. $P < 0.05$ vs vehicle group; where applicable One-Way Anova with Dunnett's post hoc test was employed.

exhibited very limited cytotoxicity in MCF-7 cell lines and thus were considered as inactive. The calculated half-maximal inhibitory dose of **6b** and **6c** was calculated as 11.9 ± 0.3 and 12.0 ± 0.4 μM, respectively.

These studies were not reported before; SBs have a versatile pharmacophore which accommodates metals quite easily in its nucleus. This study was the first report of aldehyde SBs with lamotrigine and their metal complexes and shows their potent anticonvulsant, neurotoxic, and anticancer potential. Com-

https://dx.doi.org/10.1021/acsomega.1c00027
ACS Omega 2021, 6, 7719−7730

pound **6c** was shown to possess potent activities amongst all other LTG−SB−M complexes. The potent cytotoxic agents were further used in animal models for breast cancer studies.

2.3.4. Docking Analyses. In order to delineate the mechanism of anticonvulsant and anticancer effects of the synthesized complexes, we performed molecular docking analyses.

Previous mechanistic investigations have provided evidence that the anti-epileptic effects of LTG originate from its binding at the VNaC.[13] LTG specifically blocks the sodium channel by binding to the pore in the inactivated open state. Therefore, we envisioned that the newly synthesized LTG−SB−M complexes must bind to the VNaC to elicit the anti-epileptic effect. To test this hypothesis, we docked the LTG−SB−M complex (**6c**) using the co-crystal structure of human VNaC (PDB ID: 2KAV) for calculating binding interactions. The complex **6c** also possesses the highest antiproliferative potential *in vitro*; the anticancer potential of **6c** was ascertained by analyzing its molecular docking interactions with human dihydrofolate reductase (DHFR) enzyme (PDB ID: 3GHW). For docking analyses, we used AutoDock Tools 1.5.6 15 program. Structural evaluation and validation of protein models were performed by the programs called Pyrex, Protein Ligand Interaction Profiler (PLP), and Protein plus, the best binding site prediction tools. The receptor-binding properties of different proteins along with interacting amino acid residues are reported in Table 4.

The standard drug for VNaC was LTG with amino acid residues PRO1828, LEU1829, LEU1830, ILE1831, PHE1861, and VAL1865 showing hydrophobic interactions, whereas ARG1864 was involved in ionic interactions at the binding site of 2KAV; LTG being standard shows binding energy of −5.75 Å, with 3 active torsions and inhibition constant of 61.32 along with total internal energy of −0.58 Kcal/mol as shown in Table 4. Compound **6c** shows binding energy of −10.8 Å with amino acid residues LYS1863 and GLY1870 involved in hydrogen bonding at VNaC receptor, whereas ALA1860, LYS1863, LEU1866, GLY1867, GLU1871, MET1872, and LEU1875 form hydrophobic bonds as shown in Figure 4. **6c** shows 2 active torsions and an inhibition constant of 1.19, along with total internal energy of −2.12Kcal/mol as shown in Table 4.

The drug used to standardize the results at DHFR receptor for anticancer docking studies was DOX; various parameters related to DOX are shown in Table 4 with amino acid residues VAL3, ALA9, ILE16, ASP21, LEU22, PHE31, TYR33, PHE34, GLU39, SER59, and ILE60 shows more stable docking results. Compound **6c** shows the least binding energy of −11.38 Å with the amino acid residues THR56 and SER59 involved in hydrogen bonding at the binding site of dihydrofolate enzyme, whereas ALA9, ILE16, LEU22, TRP24, GLU30, PHE34, ILE60, PRO61, VAL115, GLY117, and TYR121 were found to show hydrophobic interactions as shown in Figures 4 and 5 with 2 active torsions and inhibition constant of 4.57, along with the total internal energy of −2.14 kcal/mol as shown in Table 4.

3. CONCLUSIONS

Based on the findings of current studies, it may be inferred that the activity of lamotrigine can be enhanced by making complexes with various metals. It may also be deduced that certain metal complexes of lamotrigine derivatives have been verified as strong anticancer, anticonvulsant, and neurotoxic agents than lamotrigine alone, out of which **6c** was found to be

Table 4. Binding Properties of Receptor Proteins to Different Ligands

active compound	receptor	interacting protein (PDB ID)	efficacy	molecular formula	molecular weight (g/mol)	binding energy with receptor (kcal/mol)	inhibition constant (k_i)	no. of hydrogen bonds	interacting residues
6c	VNaC	2KAV	anticonvulsant	$C_{25}H_{19}AgCl_2N_5O_4$	632	−10.8	1.19	2	LYS1863, MET1842, ALA1860, LYS1863, LEU1866, GLY1867, GLY1870, GLU1871, MET1872, LEU1875
LTG (std.)	VNaC	2KAV	anticonvulsant	$C_9H_7Cl_2N_5$	256	−5.75	61.32	3	PRO1828, LEU1829, LEU1830, ILE1831, PHE1861, ARG1864, VAL1865
6c	DHFR	3GHW	anticancer	$C_{25}H_{19}AgCl_2N_5O_4$	632	−11.38	4.57	2	ALA9, ILE16, LEU22, TRP24, GLU30, PHE34, THR56, SER59, ILE60, PRO61, VAL115, GLY117, TYR121
DOX (std.)	DHFR	3GHW	anticancer	$C_{27}H_{29}NO_{11}$	543	−12.07	1.43	3	VAL3, ALA9, ILE16, ASP21, LEU22, PHE31, TYR33, PHE34, GLU39, SER59, ILE60

https://dx.doi.org/10.1021/acsomega.1c00027
ACS Omega 2021, 6, 7719−7730

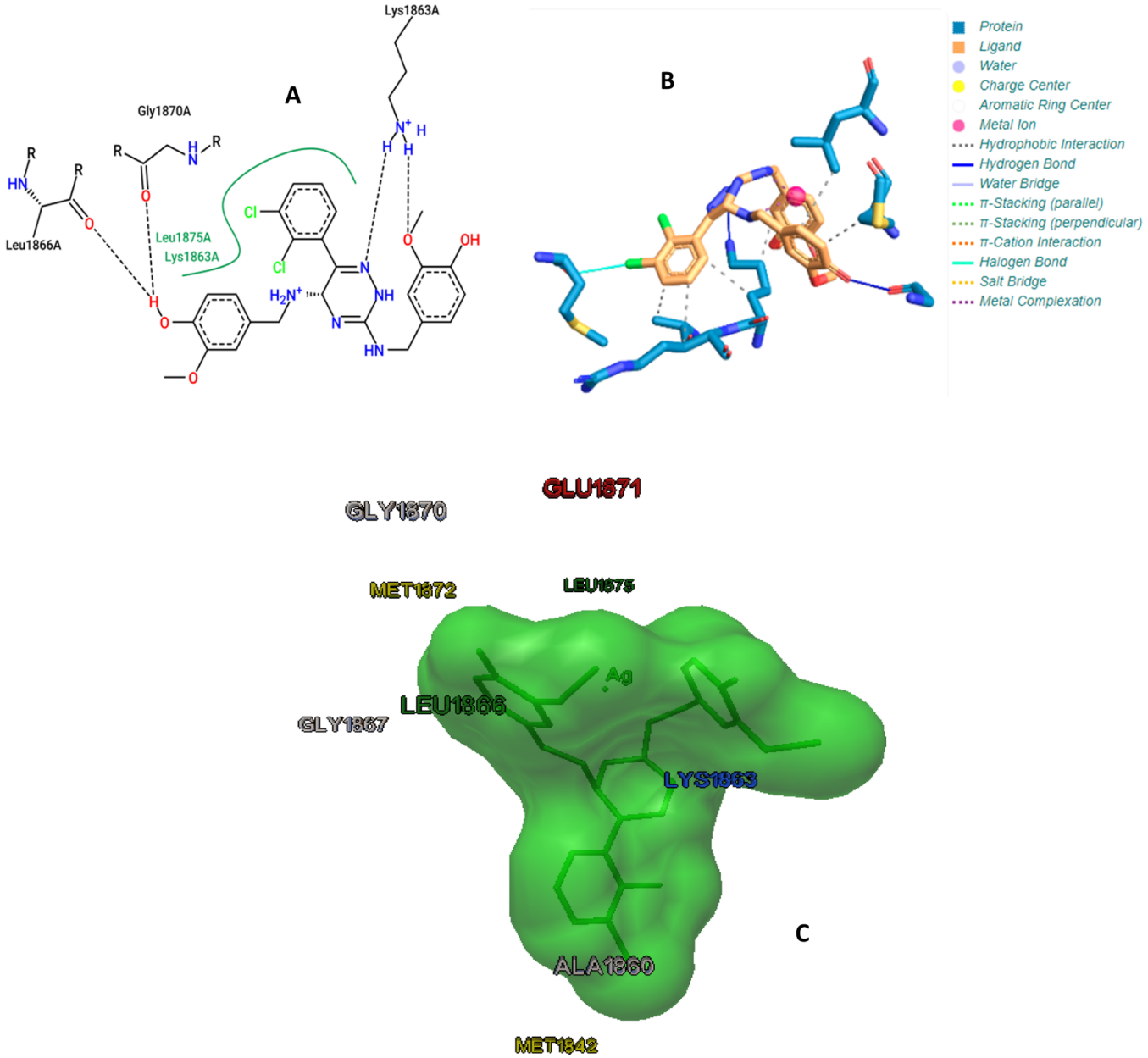

Figure 4. (A) Ligand−receptor (**6c**-2KAV) interaction (obtained from protein plus) in first conformation stabilized by two major hydrogen bonds (LYS1863 and GLY1870) with the least binding energy of docked complex and found to be −10.8 kcal/mol implies more stable docking. (B) Ligand shown in orange color with blue straight lines shows hydrogen bonding and dotted grey lines show hydrophobic interactions in the binding pocket of 2KAV receptor with residues shown in blue color. (C) Docked structure of **6c** with modeled 2KAV receptor by AutoDock; along with amino acid residues.

most significant for all activities. Synthesized metal complexes should be further verified clinically so that they may be proved for the specific potential for enhanced efficacy and reduced adverse events, which can open new ways to market. Binding mode analysis of anti-epileptic potential and antiproliferative potential has shown a fair correlation between experimental study and estimated energy of binding in **6c**.

4. EXPERIMENTAL SECTION

4.1. Materials. Lamotrigine was purchased from Stand Pharmaceuticals Pvt. Ltd., Lahore (Pakistan). All of the solvents and reagents were purchased from commercial sources and used as received unless otherwise stated. All reactions were monitored by thin layer chromatography (TLC) on precoated silica gel G-25-UV254 plates using ethyl acetate and *n*-hexane solvent system with detection under ultraviolet (UV = 254 nm) light. Melting points were recorded in degree Celsius (°C) using Dynalon SMP10 digital melting point apparatus and reported uncorrected. Infra-red (IR) spectra of conjugate-metal complexes were recorded by an Agilent FTIR spectrophotometer with the spectral region from 4000 to 400 cm^{-1}; only selected absorption maxima (ν_{max}) were reported in wavenumber (cm^{-1}). Atomic absorption spectra of ligand−metal complexes were recorded at 100−1000 mg/L. ^{1}H Nuclear magnetic resonance (NMR) spectra were recorded on a Bruker AVANCE Neo-600 spectrometer (600 MHz) using dimethyl sulfoxide (DMSO). ^{13}C NMR spectra were recorded on a Bruker AVANCE Neo-600 (150 MHz) using

https://dx.doi.org/10.1021/acsomega.1c00027
ACS Omega 2021, 6, 7719−7730

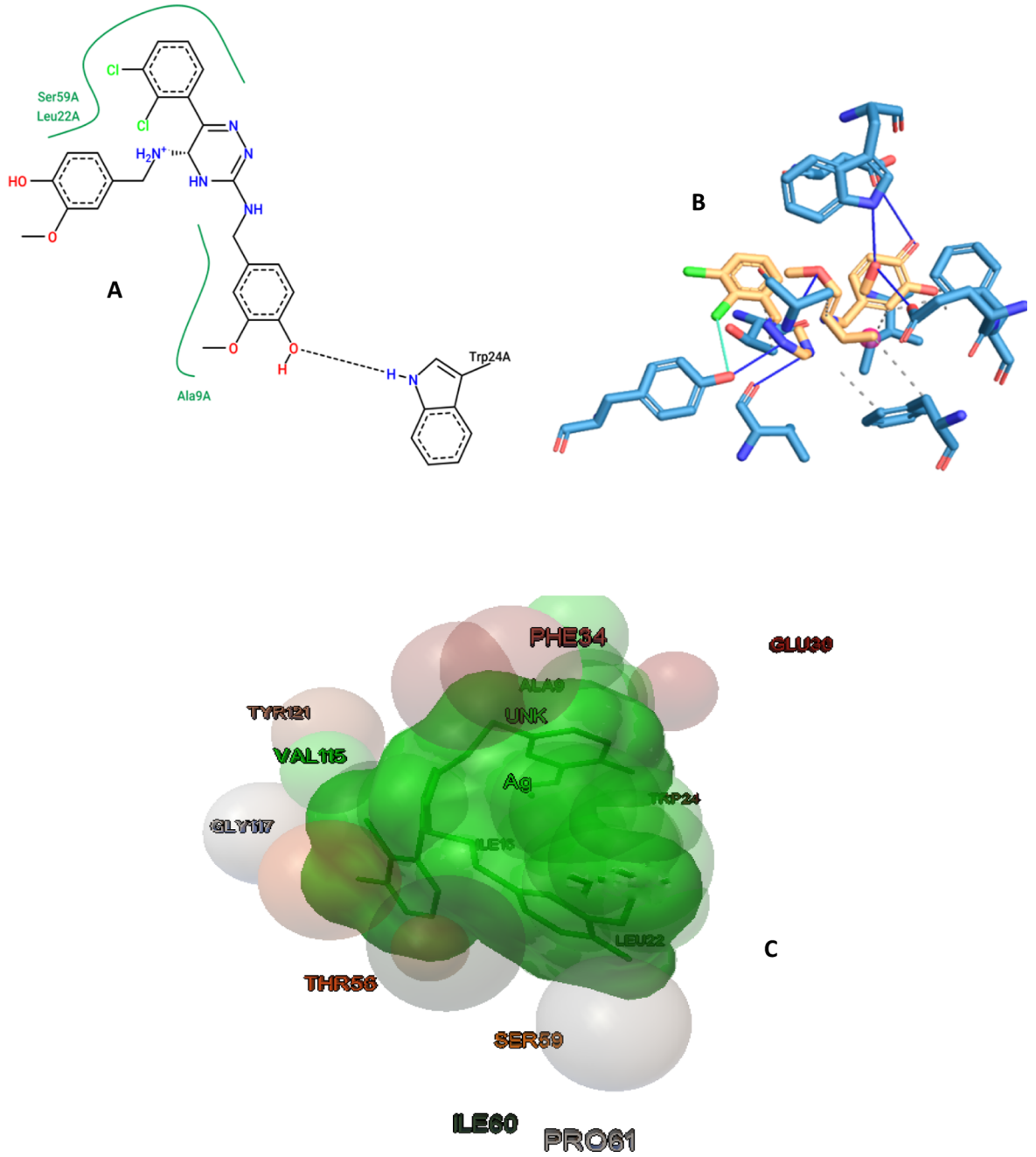

Figure 5. Docked structure of **6c** with modeled 3GHW receptor by AutoDock. (A) Ligand−receptor interaction (obtained from protein plus) in first conformation stabilized by two major hydrophobic interactions (ALA9 and LEU22) and one hydrogen bond (SER59) with the least binding energy of docked complex was found to be −11.38 kcal/mol and implies more stable docking. (B) Ligand shown in orange color with blue straight lines shows hydrogen bonding and dotted grey lines show hydrophobic interactions in the binding pocket of 3GHW receptor; blue color residues show receptor interaction with orange color ligand and (C) first conformation ligand interaction with residues of DHFR in the binding pocket of 3GHW receptor.

DMSO; chemical shifts (δ value) were referenced relative to residual protonated solvent and reported in parts per million (ppm); coupling constants (J value) were given in hertz (Hz). Electron emission mass spectra (EI-MS) were recorded on a Finnegan MAT-112 instrument. Crystal structure of the protein was obtained from Protein Data Bank. Three-dimensional structures of ligands and their metal complexes were drawn and optimized by ACD/Chem Sketch software. Molecular modeling studies were done by AutoDock 4.2.6 Tools. Compound names were generated by ChemDraw 16.0 software (PerkinElmer), following IUPAC nomenclature.

4.2. Synthetic Method. *4.2.1. General Procedure for the Synthesis of Ligands: (3_{a-c}).* Aldehyde (2 mmol) was added to lamotrigine (1 mmol) in 20 mL ethanol. A few drops of glacial acetic acid were added as catalyst. The mixture was stirred with a magnetic stirrer for a certain time as per conditions mentioned in Scheme 1. The progress of the reaction was monitored by TLC, and the final product was filtered and washed with cold water and dried at room temperature. The product so-obtained was recrystallized in chloroform/ethanol mixture.[15]

https://dx.doi.org/10.1021/acsomega.1c00027
ACS Omega 2021, 6, 7719−7730

*4.2.2. General Procedure for the Synthesis of Ligand–Metal Complexes: (**4**$_{a-c}$–**7**$_{a-c}$).* SB metal complexes were prepared by adding equimolar concentrations of the ligand and metals (1:1) in a round bottom flask along with dry toluene (30 mL) or methanol (30 mL), and triethylamine was used as a catalyst. The mixture was refluxed or stirred for several hrs according to the specified conditions as mentioned in Scheme 1. The reaction mixture was filtered off/washed and dried on a silica desiccator at room temperature or the solvent was evaporated in a rotary evaporator. The powder obtained after evaporation was recrystallized in chloroform.[12]

*4.2.3. Procedure for the Synthesis of Zinc Complexes (**4**$_{a-c}$).* 2.0 mmol of zinc chloride was dissolved in 10 mL of methanol (solution 1). 2.0 mmol of free ligand was dissolved in 10 mL of methanol (solution 2). Solution 1 was added to solution 2 with constant stirring at room temperature. The solution was stirred for 4 h at room temperature. The precipitates were filtered and washed with ice cold water and then dried on a silica desiccator at room temperature. Yellow/white colored powder/crystals were obtained. The obtained precipitates were recrystallized from chloroform and hexane mixture.

*4.2.4. Procedure for the Synthesis of Copper Complexes (**5**$_{a-c}$).* 2.0 mmol of copper (II) acetate monohydrate was dissolved in 20 mL of methanol (solution 1). 2.0 mmol of free ligand was dissolved in 20 mL of methanol (solution 2). Solution 1 was added to solution 2. The pH of the solution was adjusted to 7 by few drops of triethylamine and phosphoric acid. The solution was stirred for 4 h at room temperature. Then precipitates were filtered and allowed to dry on a silica desiccator at room temperature. Green/blue colored powder was obtained which was then washed with cold methanol for recrystallization.

*4.2.5. Procedure for the Synthesis of Silver Nitrate Complexes (**6**$_{a-c}$).* 1.0 mmol of silver nitrate was dissolved in 10 mL of methanol (solution 1). 1.0 mmol of free ligand was dissolved in 10 mL of methanol (solution 2). Solution 1 was added to solution 2 and continuously stirred at room temperature for 4 h. The precipitates were filtered and washed with ice cold water and then were dried on a silica desiccator at room temperature. Pink colored powder was obtained which was then recrystallized with ethanol.

*4.2.6. Procedure for the Synthesis of Dibutyl Tin Dichloride Complexes (**7**$_{a-c}$).* A ligand solution of 1.0 mmol was prepared in 50 mL of dry toluene. Then, triethylamine (1.0 mmol) was added to the ligand solution and refluxed for 3 h at 50 °C. Then, the reaction mixture was cooled at room temperature. Dibutyltin dichloride (1.0 mmol) was added to a flask with continuous stirring and refluxed again for 8−10 h. After completion of reflux, the mixture was filtered. The solvent was evaporated through a rotary evaporator. The precipitates obtained were recrystallized with chloroform.

*4.2.7. (1E,2Z)-N-[6-(2,3-Dichlorophenyl)-5-{(E)-[(2E)-3-phenylprop-2-en-1-ylidene]amino}-1,2,4-triazin-3-yl]prop-2-en-1-imine: (**3**$_a$).* The compound was obtained as peach-colored powder, yield: 79%, mp 112 °C; IR ν (cm^{-1}): 3328 (−NH), 3186 (Ar-CH), 2857 (=CH), 1654, 1619 (−NH), 1530, 1498 (Ar −C=C), 1151, and 1127 (−CN), 784 (−CCl); ^{1}H NMR (600 MHz, DMSO-d_6) δ (ppm): δ 7.35 (d, J = 17.6 Hz, 1H, =C**H**$_2$), 7.36 (d, J = 17.7 Hz, 1H, =N**H**), 7.45 (tdd, J = 7.4, 1.9,1.6 Hz, 1H, Ar-**H**), 7.46 (dd, J = 7.8, 1.9, 1.5, 0.4 Hz, 2H, Ar-**H**), 7.47 (dd, J = 7.8, 7.4, 1.5, 0.4 Hz, 2H, Ar-**H**), 7.48 (dd, J = 8.2, 7.9 Hz, 1H, Ar-**H**), 7.49 (dd, J = 7.8, 7.4, 1.6, 0.4 Hz, 2H, Ar-**H**), 7.50 (tdd, J = 7.4, 1.9, 1.6 Hz, 1H, Ar-**H**), 7.69 (d, J = 17.7 Hz, 1H, Ar-**H**), 7.70 (d, J = 17.7 Hz, 1H, Ar-N**H**), 7.71 (dd, J = 7.8, 1.9, 1.5, 0.4 Hz, 2H, Ar-**H**), and 7.75 (dd, J = 7.9, 1.4 Hz, 1H, Ar-**H**); ^{13}C NMR (150 MHz, DMSO-d_6) δ (ppm): δ 162.5, 154.5, 153.7, 137.2, 134.5, 132.4, 131.1, 129.2, and 128.9; EI-MS (m/z, %): 489 (0.5), 488 (3.5), 487 (13.6), 486 (20.7), 485 (69.5), 484 (31.3), and 483 (100).

*4.2.8. 2,2′-{[6-(2,3-Dichlorophenyl)-1,2,4-triazine-3,5-diyl]bis[azanylylidene(E)methanylylidene]}diphenol: (**3**$_b$).* The compound was obtained as yellow crystals, yield: 83%, mp 210 °C; IR ν (cm^{-1}): 3412 (−OH), 3317 (−NH), 3078 (Ar −CH), 2756 (=CH), 1686, 1632 (−NH), 1509 (Ar −C=C), 1155, 1116 (−CN), and 723 (−CCl); ^{1}H NMR (600 MHz, DMSO-d_6) δ (ppm): δ 7.04 (ddd, J = 8.2, 1.2, 0.5 Hz, 1H, =C**H**$_2$), 7.00 (ddd, J = 8.2, 1.2, 0.4 Hz, 1H, Ar-**H**), 7.36 (ddd, J = 7.7, 7.4, 1.2 Hz, 1H, =N**H**), 7.37 (ddd, J = 7.7, 7.4, 1.2 Hz, 2H, Ar-**H**), 7.50 (dd, J = 8.3, 7.9 Hz, 1H, Ar-**H**), 7.52 (dd, J = 8.3, 1.3 Hz, 1H, Ar-**H**), 7.70 (ddd, J = 7.7, 1.7, 0.5 Hz, 2H, Ar-N**H**), 7.72 (ddd, J = 8.2, 7.4, 1.6,0.5 Hz, 2H, Ar-**H**), and 10.26 (s, 1H, −CO**H**); ^{13}C NMR (150 MHz, DMSO-d_6) δ (ppm): δ 192.27, 162.54, 161.22, 154.61, 132.49, 132.08, 131.07, 129.73, 128.94, 119.93, and 117.70; EI-MS (m/z, %): 469 (0.3), 468 (3), 467 (13), 466 (17.9), 465 (68.7), 464 (27), and 463 (100).

*4.2.9. 4-{[(3-{(E)-[(4-Hydroxy-3-methoxyphenyl)-methylidene]amino}-6-(2,3-dichlorophenyl)-1,2,4-triazin-5-yl)imino]methyl}-2-methoxyphenol: (**3**$_c$).* The compound was obtained as white powder, yield: 78%, mp 160 °C; IR ν (cm^{-1}): 3442, 3412 (−OH), 3326 (−NH), 3058 (Ar −CH), 2737 (−CH), 1671 (−C=O), 1634 (−NH), 1586 (Ar −C=C), 1433, 1407 (−CH$_3$), 1120 (−CN), and 780 (−CCl); ^{1}H NMR (600 MHz, DMSO-d_6) δ (ppm): δ 3.37 (s, 3H, −OC**H**$_3$), 3.84 (s, 3H, −OC**H**$_3$), 6.95 (dd, J = 8.4, 0.5 Hz, 1H, =N**H**), 6.96 (dd, J = 8.2, 0.5 Hz, 1H, =C**H**$_2$), 7.35 (dd, J = 8.1, 7.9 Hz, 1H, Ar-**H**), 7.41 (dd, J = 1.6, 0.5 Hz, 1H, Ar-**H**), 7.43 (dd, J = 8.4, 1.6 Hz, 1H, Ar-**H**), 7.45 (dd, J = 8.1, 1.4 Hz, 1H, Ar-**H**), 7.69 (dd, J = 1.6, 0.5 Hz, 1H, Ar-**H**), 7.70 (dd, J = 7.9, 1.4 Hz, 1H, Ar-N**H**), 7.71 (dd, J = 8.2, 1.6 Hz, 1H, Ar-**H**), and 9.77 (s, 1H, −CO**H**); ^{13}C NMR (150 MHz, DMSO-d_6) δ (ppm): δ 162.56, 153.56, 148.64, 132.48, 131.08, 129.12, 128.93, 126.56, 115.86, 111.15, and 56.04; EI-MS (m/z, %): 529 (0.5), 528 (3.4), 527 (13.7), 526 (19.6), 525 (69.7), 524 (29.3), and 523 (100).

*4.2.10. (1E,2Z)-N-[6-(2,3-Dichlorophenyl)-5-{(E)-[(2E)-3-phenylprop-2-en-1-ylidene]amino}-1,2,4-triazin-3-yl]prop-2-en-1-imine Zinc Chloride Coordinate Complex: (**4**$_a$).* The compound was obtained as yellow crystals, yield: 99%, mp 212 °C; IR ν (cm^{-1}): 3321 (−NH), 3179 (Ar-CH), 2857 (=CH), 1654, 1619 (−NH), 1530, 1498 (Ar −C=C), 1291, 1127 (−CN), and 784 (−CCl); atomic absorption (mg/L): 0.004; EI-MS (m/z, %): 557 (0.2), 556 (1.2), 555 (5.2), 554 (9), 553 (30), 552 (26.2), 551 (74.7), 550 (37.1), 549 (100), 548 (24.7), and 547 (78.8).

*4.2.11. 2,2′-{[6-(2,3-Dichlorophenyl)-1,2,4-Triazine-3,5-Diyl]bis[azanylylidene(E)methanylylidene]}diphenol Zinc Chloride Coordinate Complex: (**4**$_b$).* The compound was obtained as yellow powder, yield: 90%, mp 205 °C; IR ν (cm^{-1}): 3501 (−OH), 3352 (−NH), 3104 (Ar −CH), 1669, 1619 (−NH), 1533, 1518 (Ar −C=C), 1146, 1110 (−CN), 915 (=CH), and 739 (−CCl); atomic absorption (mg/L): 0.137; EI-MS (m/z, %): 537 (0.2), 536 (1.1), 535 (4.9), 534 (7.8), 533 (29.3), 532 (23.3), 531 (74), 530 (33.1), 529 (100), 528 (21.4), and 527 (79.3).

https://dx.doi.org/10.1021/acsomega.1c00027
ACS Omega 2021, 6, 7719−7730

*4.2.12. 4-{[(3-{(E)-[(4-Hydroxy-3-methoxyphenyl)-methylidene]amino}-6-(2,3-dichlorophenyl)-1,2,4-triazin-5-yl)imino]methyl}-2-methoxyphenol Zinc Chloride Coordinate Complex: (**4$_c$**).* The compound was obtained as off-white crystals, yield: 115%, mp 105 °C; IR ν (cm^{-1}): 3309 (−NH), 3201 (−OH), 3018 (Ar −CH), 2756 (−CH), 1623 (−NH), 1496, 1484 (Ar −C═C), 1436, 1410 ($-CH_3$), 1295 (−C−O), 1153, 1114 (−CN), and 782 (−CCl); atomic absorption (mg/L): 0.74; EI-MS (*m*/*z*, %): 599 (0.2), 598 (1.2), 597 (1.5), 596 (8.5), 595 (29.9), 594 (25), 593 (74.6), 592 (35.3), 591 (100), 590 (23.1), and 589 (78.7).

*4.2.13. (1E,2Z)-N-[6-(2,3-Dichlorophenyl)-5-{(E)-[(2E)-3-phenylprop-2-en-1-ylidene]amino}-1,2,4-triazin-3-yl]prop-2-en-1-imine Copper Acetate Coordinate Complex: (**5$_a$**).* The compound was obtained as sea-green powder, yield: 70%, mp decompose at high temp.; IR ν (cm^{-1}): 3321 (−NH), 3181 (Ar-CH), 2857 (═CH), 1653, 1619 (−NH), 1530, 1498 (Ar −C═C), 1291, 1127 (−CN), and 784 (−CCl); atomic absorption (mg/L): 0.16; EI-MS (*m*/*z*, %): 554 (0.2), 553 (1.4), 552 (5.7), 551 (11.1), 550 (39), 549 (30.4), 548 (100), 547 (27.4), and 546 (87.7).

*4.2.14. 2,2′-{[6-(2,3-Dichlorophenyl)-1,2,4-triazine-3,5-diyl]bis[azanylylidene(E)methanylylidene]}diphenol Copper Acetate Coordinate Complex: (**5$_b$**).* The compound was obtained as olive green powder, yield: 94%, mp decompose at high temp.; IR ν (cm^{-1}): 3481 (−OH), 3367 (−NH), 3054, 3013 (Ar −CH), 1632, 1604 (−NH), 1524, 1430 (Ar −C═C), 1190, 1148 (−CN), 900 (═CH), and 732 (−CCl); atomic absorption (mg/L): 1.183; EI-MS (*m*/*z*, %): 534 (0.1), 533 (1.2), 532 (5.4), 531 (9.6), 530 (38.5), 529 (26.4), 528 (100), 527 (23.8), and 526 (88.3).

*4.2.15. 4-{[(3-{(E)-[(4-Hydroxy-3-methoxyphenyl)-methylidene]amino}-6-(2,3-dichlorophenyl)-1,2,4-triazin-5-yl)imino]methyl}-2-methoxyphenol Copper Acetate Coordinate Complex: (**5$_c$**).* The compound was obtained as brown crystals, yield: 60%, mp decompose at high temp.; IR ν (cm^{-1}): 3315 (−NH), 3183 (Ar −CH), 2292, 2111 (−OH), 1619 (−NH), 1573, 1559 (Ar −C═C), 1464 ($-CH_2$), 1431 ($-CH_3$), 1228 (−C−O), 1114, 1019 (−CN), and 780 (−CCl). Atomic absorption (mg/L): 1.338; EI-MS (*m*/*z*, %): 596 (0.1), 595 (1.3), 594 (5.7), 593 (10.5), 592 (39.1), 591 (28.6), 590 (100), 589 (25.7), and 588 (87.5).

*4.2.16. (1E,2Z)-N-[6-(2,3-Dichlorophenyl)-5-{(E)-[(2E)-3-phenylprop-2-en-1-ylidene]amino}-1,2,4-triazin-3-yl]prop-2-en-1-imine Silver Nitrate Coordinate Complex: (**6$_a$**).* The compound was obtained as peach-colored powder, yield: 68%, mp 210 °C; IR ν (cm^{-1}): 3308 (−NH), 3147 (Ar-CH), 2867 (═CH), 1625, 1619 (−NH), 1559, 1507 (Ar −C═C), 1310, 1157 (−CN), and 719 (−CCl); EI-MS (*m*/*z*, %): 598 (0.3), 597 (2), 596 (8.1), 595 (14), 594 (48.1), 593 (30.7), 592 (100), 591 (19.3), and 590 (61.6).

*4.2.17. 2,2′-{[6-(2,3-Dichlorophenyl)-1,2,4-triazine-3,5-diyl]bis[azanylylidene(E)methanylylidene]}diphenol Silver Nitrate Coordinate Complex: (**6$_b$**).* The compound was obtained as white powder, yield: 69%, mp 215 °C; IR ν (cm^{-1}): 3501 (−OH), 3315 (−NH), 3201 (Ar −CH), 1626 (−NH), 1559, 1507 (Ar −C═C), 1167, 1112 (−CN), 915 (═CH), and 719 (−CCl); EI-MS (*m*/*z*, %): 578 (0.2), 577 (1.7), 576 (7.6), 575 (12.1), 574 (47.5), 573 (26.6), 572 (100), 571 (16.7), and 570 (61.9).

*4.2.18. 4-{[(3-{(E)-[(4-Hydroxy-3-methoxyphenyl)-methylidene]amino}-6-(2,3-dichlorophenyl)-1,2,4-triazin-5-yl)imino]methyl}-2-methoxyphenol Silver Nitrate Coordinate Complex: (**6$_c$**).* The compound was obtained as tea-pink powder, yield: 103%, mp 205 °C; IR ν (cm^{-1}): 3412 (−OH), 3319 (−NH), 3186 (Ar −CH), 1627 (−NH), 1559, 1507 (Ar −C═C), 1313 (−C−O), 1151, 1112 (−CN), and 750 (−CCl); EI-MS (*m*/*z*, %): 638 (0.3), 637 (1.9), 636 (8.1), 635 (13.2), 634 (48.2), 633 (28.8), 632 (100), 631 (18), and 630 (61.5).

*4.2.19. (1E,2Z)-N-[6-(2,3-Dichlorophenyl)-5-{(E)-[(2E)-3-phenylprop-2-en-1-ylidene]amino}-1,2,4-triazin-3-yl]prop-2-en-1-imine Dibutyl Tin Dichloride Coordinate Complex of L1: (**7$_a$**).* The compound was obtained as off-white powder, yield: 74%, mp decompose at high temp.; IR ν (cm^{-1}): 3308 (−NH), 3158 (Ar-CH), 2939 (═CH), 1656, 1636 (−NH), 1597, 1559 (Ar −C═C), 1295, 1032 (−CN), and 721 (−CCl); EI-MS (*m*/*z*, %): 703 (0.1), 702 (0.4), 701 (1.5), 700 (2.9), 699 (8.6), 698 (8.4), 697 (25), 696 (21.7), 695 (59.6), 694 (46.3), 693 (100), 692 (47.4), 691 (66), 690 (23.2), and 689 (25.7).

*4.2.20. 2,2′-{[6-(2,3-Dichlorophenyl)-1,2,4-triazine-3,5-diyl]bis[azanylylidene(E)methanylylidene]}diphenol Dibutyl Tin Dichloride Coordinate Complex: (**7$_b$**).* The compound was obtained as white powder, yield: 120%, mp 205 °C; IR ν (cm^{-1}): 3447 (−OH), 3300 (−NH), 3203 (Ar −CH), 1656, 1636 (−NH), 1559, 1530 (Ar −C═C), 1410 ($-CH_3$), 1295, 1158 (−CN), 916 (═CH), and 717 (−CCl); EI-MS (*m*/*z*, %): 675 (0.1), 674 (0.4), 673 (1.5), 672 (2.7), 671 (8.5), 670 (7.9), 669 (24.8), 668 (20.6), 667 (59.2), 666 (44.5), 665 (100), 664 (46.3), 663 (66.1), 662 (22.9), and 661 (25.9).

*4.2.21. 4-{[(3-{(E)-[(4-Hydroxy-3-methoxyphenyl)-methylidene]amino}-6-(2,3-dichlorophenyl)-1,2,4-triazin-5-yl)imino]methyl}-2-methoxyphenol Dibutyl Tin Dichloride Coordinate Complex: (**7$_c$**).* The compound was obtained as off-white powder, yield: 82%, mp decompose at high temp.; IR ν (cm^{-1}): 3445 (−OH), 3304 (−NH), 3054 (Ar −CH), 1656 (−C═O), 1634 (−NH), 1489 (Ar −C═C), 1403 ($-CH_3$), 1295 (−C−O), 1153, 1032 (−CN), and 723 (−CCl); EI-MS (*m*/*z*, %): 767 (0.1), 766 (0.4), 765 (1.6), 764 (2.8), 763 (8.7), 762 (8.5), 761 (25.3), 760 (21.9), 759 (60), 758 (46.5), 757 (100), 756 (47.4), 755 (65.8), 754 (23.1), and 753 (25.5).

4.3. Solubility Studies. Apparent solubility of all synthesized metal complexes was determined. A measured amount of metal complexes was dissolved in a weighed amount of solvent and clarity of the solution was observed. Water, methanol, ethanol, DMSO, and chloroform were used for this study. For good solubility, the threshold value of <0.1/100 mL with the clear-colored solution in the given solvent was considered.[16]

4.4. Molecular Modeling. *4.4.1. Receptor and Ligand Selection.* Docking studies were carried out using AutoDock 4.2 program.[17] Three-dimensional (3D) crystal structure of the enzyme was retrieved from RCSB Protein Data Bank (PDB) with PDB-ID: 2KAV (https://www.rcsb.org/structure/2KAV) for anticonvulsant activity and PDB-ID: 3GHW (https://www.rcsb.org/structure/3GHW) for antitumor activity. Two-dimensional (2D) structures of [3,5-diamine-6-(2,3-dichlorophenyl)-1,2,4-triazine] metal complexes were drawn and optimized by ACD/Chem Sketch software and saved as an MDL file. The MDL files were 3D protonated and energy minimized to PDB by using Open Babel GUI.[14] The 2D structures of the ligand are shown in Table 1. Crystal structures of 2KAV and 3GHW were modeled using AutoDock Tools 1.5.6; the impurities were removed, whereas partial charges and polar hydrogen were added. The macromolecule was saved

https://dx.doi.org/10.1021/acsomega.1c00027
ACS Omega 2021, 6, 7719−7730

in its respective PDBQT format for ligand interactions.[18] The best active region of the enzyme was selected by targeting a binding site with amino acid residues involved in binding to a ligand.[19]

4.4.2. Homology Modeling. Computer-aided drug design provides the platform to understand receptor and ligand interactions. Docking is a well-established computational technique used to predict interactions between a receptor and newly designed compounds.[20] Molecular docking and scoring of 2KAV and 3GHW receptors was computed by AutoDock 4.2 software; it simulates the binding conformations of the ligand on VNaC for anticonvulsant activity and dihydrofolate enzyme for antitumor action and elicits the binding sites of the docked molecule utilizing Lamarckian Genetic Algorithm (LGA). The grid box was set at 110 × 100 × 100 Å along *X*, *Y*, and *Z* axes with a grid spacing of 0.375 Å to recognize the binding site of the ligand. The AutoDock parameters used were genetic algorithm with population size = 150; maximum number of energy evaluations = 250,000; and genetic algorithm cross-over mode = 2 points. The rigidity parameters were set for the receptor, keeping the ligand flexible. Ten docked orientations (poses) were obtained after protein−ligand docking at 2KAV and 3GHW receptors. The best conformations were screened in terms of the lowest binding energy among several bioactive conformations generated by various interactions. Cluster analysis of protein-binding sites with the lowest binding energy was further explored using Pymol Molecular Graphics System offline software and Protein Plus and Protein−Ligand Interacting Profile (PLP) online software.[2,20]

4.4.3. Model Validation. The reliability of the docking program was validated by using the redocking method; in both cases, the co-crystallized ligands were redocked in the active site of the enzyme. Root mean square deviation (rmsd) was then calculated, and in all cases, rmsd value of <2.0 Å was considered accurate in predicting binding orientation of ligand.[16]

4.5. *In Vitro* Cytotoxicity. Cytotoxic activity of compounds was evaluated in 96-well flat-bottomed microplates by using the standard MTT (3-[4,5-dimethylthiazole-2-yl]-2,5-diphenyl-tetrazolium bromide) colorimetric assay.[21] For this purpose, MCF-7 cells (breast cancer) were cultured in Eagle's minimum essential medium, supplemented with 10% fetal bovine serum, 1% penicillin/streptomycin, a non-essential amino acid (0.1 mM), insulin (10 μg/mL), and sodium pyruvate (1 mM) in 75 cm^2 flasks, with the temperature maintained at 37 °C in humidified and concentrated 5% CO_2 atmosphere. 2−3 mL of warm trypsin (0.25%) and ethylenediaminetetraacetate solution (0.53 mM) were added to cells to detach the cell layer, the growing cells were harvested and counted with a hemocytometer. Once the MCF-7 cell layer was detached, trypsin was neutralized by adding 10 mL of complete growth medium to a flask and the cells were suspended by gentle pipetting. Trypsin/growth medium suspension was aspirated from the tube. MCF-7 cell pellet was suspended again in 10 mL of fresh growth medium.

Cell culture with the concentration of 6×10^4 cells/mL was prepared and introduced (100 μL/well) into 96-well plates. After overnight incubation, the medium was removed and 200 μL of fresh medium was added with different concentrations of compounds (1−30 μM). After 48 h, 200 μL of MTT (0.5 mg/mL) was added to each well and incubated further for 4 h. Subsequently, 100 μL of DMSO was added to each well.[22] The extent of MTT reduction to formazan within cells was calculated by measuring the absorbance at 570 nm, using a microplate reader (Spectra Max plus, Molecular Devices, CA, USA). The cytotoxicity was recorded as concentration causing 50% growth inhibition (IC50) for MCF-7. The percentage inhibition was calculated by using the following formula

$$\%\ \text{inhibition} = 100 - ((\text{mean of O. D of test compound} - \text{mean of O. D of negative control})/(\text{mean of O. D of positive control} - \text{mean of O. D of negative control}) \times 100)$$

The results (% inhibition) were processed by using Soft-Max Pro software (Molecular Device, USA).

4.6. Anticonvulsant Activity. *4.6.1. Experimental animals.* In this experiment, white Albino mice of either sex (male or female), 8−10 weeks old, weighing about 25−35 g were considered. The animals were kept in iron cages under standard conditions at 25 °C with 45−65 percent relative humidity on 12 h of light and dark cycle. The mice had free access to food and water. The experimental protocol was recommended and approved by the research and ethical committee (REC) of the Riphah Institute of Pharmaceutical Sciences, Islamabad—Pakistan (approval ID: ref. no. REC/RIPS/2019/09 and Date of Approval: 28th Nov, 2019) and approved protocols were strictly adhered to for the PTZ convulsion model and minimal motor impairment (MMI) model with minor modifications.[7,23]

4.6.2. Anticonvulsant Model. For this model, overnight fasted mice were randomly assigned to 6 groups (n = 10), weighed, and marked. Group-I was considered a controlled group as it received a blank solution [carboxy methylcellulose (CMC)] without the drug. Group-II was considered a negative control group as it received PTZ 70 mg/kg, whereas group-III was considered as a reference as it received the standard anticonvulsant drug lamotrigine (LTG). Group-IV to group-VI were considered as treated groups as they received newly synthesized anticonvulsant agents (5 mg/kg) suspended in CMC and sonicated for few hours before i.p injection.

The anticonvulsant effects of PTZ for the generation of clonic convulsions in monotherapy were estimated at doses of 30, 40, 50, 60, and 70 mg/kg. The anticonvulsant effects of LTG in monotherapy were estimated at doses of 1, 2, 3, 4, and 5 mg/kg against clonic convulsions induced by PTZ. For each antiepileptic drug used in monotherapy, the highest non-protective dose was established in the laboratory with the following criteria: (i) it was the highest dose unable to protect 10% of mice against PTZ, (ii) it was the highest dose that does not produce statistically significant results. The highest nonprotective dose of LTG in the PTZ model was 5 mg/kg (6% of mice were protected from clonic convulsions). After dose administration, the mice were observed for 30 min for latency of convulsions, duration of convulsions, and seizure score. The intensity of seizures was evaluated using a 6-point scale, taking as a basis the following criteria (including the number of animals that died):[24] 0—no response, 1—ear and facial twitching, 2—axial convulsive wave throughout the body, 3—myoclonic body jerks, 4—generalized clonic convulsions, 5—generalized convulsions with tonic extensions, 6—mortality or death.

4.7. Neurotoxicity or MMI. Neurotoxicity was studied in animals already administered with convulsive doses by

https://dx.doi.org/10.1021/acsomega.1c00027
ACS Omega 2021, 6, 7719−7730

intraperitoneal injection of the synthesized drug. In this study, animals were trained to balance on a rotating rod 2.5 cm diameter and 25 cm high. The animals were placed in isolation cages and observed for the next 30 min for the presence or absence of an episode of clonic spasm persisting for at least 5 s. The absence of seizures suggests that the test compound has the ability to raise the seizure threshold. All animals were subjected to rotarod test after 30 min of intraperitoneal injection of synthesized compounds and again after 4 h of intraperitoneal injection. Neurotoxicity was determined by the inability of the animal to remain on the rod for 1 min. Test substances also appeared to have a rapid onset and short duration of action because both anticonvulsant and neurotoxic effects were greater at 30 min than 4 h.[7,23]

4.8. Statistical Analysis. All results were represented as mean ± standard error of the mean (SEM). Analysis of variance was performed, where appropriate One-Way ANOVA followed by post-hoc Dunnet's test was employed using GraphPad Prism-9. $*P < 0.05$, $**P < 0.01$, and $***P < 0.001$ were considered as level of significance, low significance, moderate significance, and highly significant, respectively.

■ ASSOCIATED CONTENT

Supporting Information

The Supporting Information is available free of charge at https://pubs.acs.org/doi/10.1021/acsomega.1c00027.

FTIR, ^{1}H NMR, ^{13}C NMR spectra, EI-MS, and atomic absorption spectra of compounds (PDF)

■ AUTHOR INFORMATION

Corresponding Authors

Saima Najm − *Faculty of Pharmaceutical Sciences, Riphah International University, Islamabad 44000, Pakistan; Faculty of Pharmacy, Lahore College of Pharmaceutical Sciences, Lahore 55150, Pakistan;* orcid.org/0000-0002-2588-7037; Email: saminajm@hotmail.com

Muhammad Saeed − *Department of Chemistry and Chemical Engineering, Syed Babar Ali School of Science and Engineering, Lahore University of Management Science, Lahore 54792, Pakistan*; Email: Muhammad.saeed@lums.edu.pk

Authors

Humaira Naureen − *Faculty of Pharmaceutical Sciences, Riphah International University, Islamabad 44000, Pakistan*

Kishwar Sultana − *Faculty of Pharmacy, The University of Lahore, Lahore 54590, Pakistan*

Fareeha Anwar − *Riphah Institute of Pharmaceutical Sciences, Lahore 55150, Pakistan;* orcid.org/0000-0001-5097-8128

Muhammad Mubbashir Khan − *Faculty of Pharmacy, The University of Lahore, Lahore 54590, Pakistan*

Humaira Nadeem − *Faculty of Pharmaceutical Sciences, Riphah International University, Islamabad 44000, Pakistan*

Complete contact information is available at: https://pubs.acs.org/10.1021/acsomega.1c00027

Notes

The authors declare no competing financial interest.

■ ACKNOWLEDGMENTS

The authors are grateful to Riphah Institute of Pharmaceutical Sciences for grants for purchasing chemicals. They also acknowledge M.M.K. (Quality Control Manager), Briell Pharmaceuticals (Pvt.) Ltd, Lahore-Pakistan, for his skillful assistance in recording FTIR. Thanks are also due to K.S., Faculty of Pharmacy, The University of Lahore, Lahore, Pakistan, for providing laboratory facilities and practical support. The authors also acknowledge M.S., Department of Chemistry and Chemical Engineering, Syed Babar Ali School of Science and Engineering, Lahore University of Management Science, Lahore, Pakistan, for his skillful assistance in the characterization of compounds.

■ REFERENCES

(1) Najib, F. M.; Mustafa, M. S. Spectrophotometric methods for simultaneous determination of carbamazepine and lamotrigine in binary mixtures and urine samples. *Malaysian J. Anal. Sci.* **2014**, *18*, 491−506.

(2) Poureshghi, F.; Ghandforoushan, P.; Safarnejad, A.; Soltani, S. Interaction of an antiepileptic drug, lamotrigine with human serum albumin (HSA): application of spectroscopic techniques and molecular modeling methods. *J. Photochem. Photobiol.* **2017**, *166*, 187−192.

(3) Vallés, A. S.; Garbus, I.; Barrantes, F. J. Lamotrigine is an open-channel blocker of the nicotinic acetylcholine receptor. *NeuroReport* **2007**, *18*, 45−50.

(4) Kim, K. J.; Jeun, S. H.; Sung, K.-W. Lamotrigine, an antiepileptic drug, inhibits 5-HT3 receptor currents in NCB-20 neuroblastoma cells. *Korean J. Physiol. Pharmacol.* **2017**, *21*, 169−177.

(5) Sudhakar, K.; Meda, R. In vitro anticancer activity of lamotrigine and 5-fluorouracil individually and in combination on human K562 and COLO320HSR cell lines by trypan blue assay. *Int. J. Pharm. Biol. Sci.* **2014**, *5*, 387−393.

(6) Pellegrino, M.; Rizza, P.; Nigro, A.; Ceraldi, R.; Ricci, E.; Perrotta, I.; Aquila, S.; Lanzino, M.; Ando, S.; Morelli, C.; Sisci, D. FoxO3 mediates the inhibitory effects of the antiepileptic drug lamotrigine on breast cancer growth. *Mol. Canc. Res.* **2018**, *16*, 923−934.

(7) Cuadrado, A.; Bravo, J.; Armijo, J. A. Synergistic interaction between felbamate and lamotrigine against seizures induced by 4-aminopyridine and pentylenetetrazole in mice. *Eur. J. Pharmacol.* **2003**, *465*, 43−52.

(8) Sinha, S. K.; Shrivastava, P. K.; Shrivastava, S. K. Synthesis, characterization, and biological activity of three new amide prodrugs of lamotrigine with reduced hepatotoxicity. *Chem. Pap.* **2011**, *65*, 70−76.

(9) Hlavác, J.; Buchtík, R.; Slouka, J.; Hradil, P.; Wiedermannová, I. Synthesis of oxo analogs of lamotrigine and related compounds. *Arkivoc* **2003**, *2003*, 22−28.

(10) Qian, Y.; Lv, P.-C.; Shi, L.; Fang, R.-Q.; Song, Z.-C.; Zhu, H.-L. Synthesis, antimicrobial activity of lamotrigine and its ammonium derivatives. *J. Chem. Sci.* **2009**, *121*, 463−470.

(11) Khan, M. A.; Akhtar, S.; Shahid, K. Synthesis, characterization and in-vitro biological assays of triphenyltin derivatives of phenyl hydrazones. *Int. J. Pharm. Sci.* **2014**, *28*, 147−151.

(12) Akhtar, S.; Abbas, M.; Shahid, K.; Akhtar, H. Metal complexes of ribavirin; synthesis, characterization and in-vitro biological screening. *Int. J. Pharm. Sci. Res.* **2018**, *9*, 1666−1672.

(13) Cronin, N. B.; O'Reilly, A.; Duclohier, H.; Wallace, B. A. Binding of the anticonvulsant drug lamotrigine and the neurotoxin batrachotoxin to voltage-gated sodium channels induces conformational changes associated with block and steady-state activation. *J. Biol. Chem.* **2003**, *278*, 10675−10682.

(14) Morris, G. M.; Huey, R.; Lindstrom, W.; Sanner, M. F.; Belew, R. K.; Goodsell, D. S.; Olson, A. J. AutoDock4 and AutoDockTools4:

Automated docking with selective receptor flexibility. *J. Comput. Chem.* **2009**, *30*, 2785−2791.
(15) Xavier, D. A.; Srividhya, N.; Srividhya, N. Synthesis and study of Schiff base ligands. *J. Appl. Chem.* **2014**, *7*, 06−15.
(16) Jabeen, M.; Ahmad, S.; Shahid, K.; Sadiq, A.; Rashid, U. Ursolic Acid Hydrazide Based Organometallic Complexes: Synthesis, Characterization, Antibacterial, Antioxidant, and Docking Studies. *J. Front. Chem.* **2018**, *6*, 55−65.
(17) Morris, G. M.; Goodsell, D. S.; Robert, S. H.; Ruth, H.; William, E. H.; Richard, K. B.; Arthur, J. O. Automated Docking Using a Lamarckian Genetic Algorithm and an Empirical Binding Free Energy Function. *J. Comput. Chem.* **1998**, *19*, 1639−1662.
(18) Yang, J.; Roy, A.; Zhang, Y. Protein-ligand binding site recognition using complementary binding specific substructure comparison and sequence profile alignment. *J. Bioinf.* **2013**, *29*, 2588−2595.
(19) Ebrahimipour, S. Y.; Sheikhshoaiea, I.; Castrob, J.; Dusekc, M.; Tohidiana, Z.; Eignerc, V.; Khaleghi, M. Synthesis, spectral characterization, structure studies, molecular docking and antimicrobial evaluation of new dioxidouranium(VI) complexes incorporating tetradentate N_2O_2 Schiff base ligands. *RSC Adv.* **2015**, *9*, 95104−95117.
(20) Mahmoud, W. H.; Deghadi, R. G.; Mohamed, G. G. Metal complexes of ferrocenyl-substituted Schiff base: Preparation, characterization, molecular structure, molecular docking studies and biological investigation. *J. Organomet. Chem.* **2020**, *2*, 121113.
(21) Venugopal, K.; Ahmad, H.; Manikandan, E.; Thanigai Arul, K.; Kavitha, K.; Moodley, M. K.; Rajagopal, K.; Balabhaskar, R.; Bhaskar, M. The effect of anticancer activity upon Beta Vulgaris extract mediated biosynthesized silver nanoparticles against human breast (MCF-7), lungs (A549) and pharynx (Hep-2) cancer cell lines. *J. Photochem. Photobiol., B* **2017**, *173*, 99−107.
(22) Wang, X.; Teng, Z.; Wang, H.; Wang, C.; Liu, Y.; Tang, Y.; Wu, J.; Sun, J.; Wang, H.; Wang, J.; Lu, G. Increasing the cytotoxicity of doxorubicin in breast cancer MCF-7 cells with multidrug resistance using a mesoporous silica nanoparticle drug delivery system. *Int. J. Clin. Exp. Pathol.* **2014**, *7*, 1337−1347.
(23) Wang, S.; Liu, H.; Wang, X.; Lei, K.; Li, G.; Li, J.; Liu, R.; Quan, Z. Synthesis of 1,3,4-oxadiazole derivatives with anticonvulsant activity and their binding to the GABAA receptor. *Eur. J. Med. Chem.* **2020**, *206*, 112672.
(24) Gerald, M. C.; Riffee, W. H. Acute and chronic effects of d- and l-amphetamine on seizure susceptibility in mice. *Eur. J. Pharmacol.* **1973**, *21*, 323−330.

https://dx.doi.org/10.1021/acsomega.1c00027
ACS Omega 2021, 6, 7719−7730